Comparison of $YBa_2Cu_{3-x}Zn_xO_7$ and $Er_{1-y}Pr_yBa_2Cu_3O_7$ systems: Raman and XPS studies

In-Sang Yang and Y. J. Wee
Department of Physics, Ewha Woman's University, Seoul 120-750, Korea

S.-J. Kim
Department of Chemistry, Ewha Woman's University, Seoul 120-750, Korea

Kyun Nahm and Chul Koo Kim
Department of Physics, Yonsei University, Seoul 120-749, Korea

Moonsup Han, W. C. Yang, and S.-J. Oh
Department of Physics, Seoul National University, Seoul 151-742, Korea
(Received 17 August 1992; revised manuscript received 17 February 1993)

We report results of Raman and x-ray photoemission spectroscopy (XPS) measurements of the $YBa_2Cu_{3-x}Zn_xO_7$ and $Er_{1-y}Pr_yBa_2Cu_3O_7$ systems. No appreciable changes were observed for $YBa_2Cu_{3-x}Zn_xO_7$ in either measurement. On the other hand, Raman frequencies of Ba and apical oxygen (O_z) modes increase and the binding energies of Ba core levels show an increasing trend as y increases in $Er_{1-y}Pr_yBa_2Cu_3O_7$. Results for $Er_{1-y}Pr_yBa_2Cu_3O_7$ are consistent with our prevous work for Pr-doped 1:2:3 superconductors and can be explained in terms of hole localization at Ba sites. Our experimental results indicate that the suppression mechanism in the $YBa_2Cu_{3-x}Zn_xO_7$ system is different from that in the $Er_{1-y}Pr_yBa_2Cu_3O_7$ system.

I. INTRODUCTION

Since the discovery of a particular class of high-temperature superconductors by Bednorz and Müller,[1] there have been numerous experimental and theoretical studies on these materials. These studies include a substantial number of Raman[2] and x-ray photoemission spectroscopy[3] (XPS) investigations. Such studies could prove to be informative since vibrational spectroscopy is a sensitive probe for changes in crystal structure[4] and XPS for changes in electronic structure.[5] These changes seem to play an important role in determining the superconductivity of high-temperature superconductors.

We report Raman and XPS measurements on well-characterized $YBa_2Cu_{3-x}Zn_xO_7$ ($x=0.0$, 0.025, 0.06, 0.09, hereafter Y-Zn 1:2:3) and $Er_{1-y}Pr_yBa_2Cu_3O_7$ ($y=0.0$, 0.1, 0.2, 0.3, 0.4, hereafter Er-Pr 1:2:3) systems. The superconducting transition temperature T_c of both systems is known to be suppressed as x (Ref. 6) and y (Ref. 7) increase, respectively. However, the suppression mechanism in both systems is not clearly understood yet. The specific reason that we choose these systems is explained in the following paragraphs. In this paper, we would like to compare the substitution effects in (1:2:3)-type superconductors by Zn for Cu sites and by Pr for Y sites.

The substitution of Cu in $YBa_2Cu_3O_7$ (Y 1:2:3) by the transition metal elements systematically suppresses T_c, regardless of magnetic characters of the substituted ions.[8] In particular, substitution by Zn suppresses T_c most. The divalent Zn ion is nonmagnetic and believed to occupy the Cu(2) site at low concentration.[9] Several mechanisms have been proposed for the suppression of T_c including disordering of the CuO_2 planes[10] and increasing hole concentration.[6]

Also the effects of the substitution of Y sites in (1:2:3)-type superconductors have been studied systematically for all rare-earth elements.[7] Among (L)1:2:3, which has the same structure as Y 1:2:3, where L is a lanthanide element, only Pr 1:2:3 is not superconducting. Thus Pr 1:2:3 has been studied widely with the hope of understanding better the mechanism of superconductivity. $Y_{1-x}Pr_xBa_2Cu_3O_7$ (Y-Pr 1:2:3) is a solid solution that has the same structure as Y 1:2:3, yet T_c is suppressed as the Pr concentration increases. The mechanism for suppression of superconductivity in this compound is still in debate. In our previous paper, the Ba core-level shifts have been reported in XPS measurements on the Y-Pr 1:2:3 system.[11] Raman measurements on the Y-Pr 1:2:3 system showed that the Ba and O_z modes shifted to higher frequencies.[12] From these shifts we suggested that holes may become localized at Ba sites as the Pr concentration increases in Y-Pr 1:2:3.[13]

In this study, we want to compare Y-Zn 1:2:3 and Er-Pr 1:2:3 systems. The former has disturbance in CuO_2 planes, the latter has disturbance in the Y sites of (1:2:3)-type superconductors. Thereby, we would like to find out whether there is a difference in the mechanism for suppression of superconductivity of both systems. The reason that we choose Er-Pr 1:2:3 is that the Er^{3+} ion has stronger magnetic moment ($\mu_{\text{eff}}=9.5\mu_B$) than the Pr^{3+} ion ($\mu_{\text{eff}}=3.5\mu_B$), yet Er-Pr 1:2:3 shows similar suppression behavior as Y-Pr 1:2:3. We want to observe the Raman and XPS spectra of Er-Pr 1:2:3 to see if there is simi-

lar behavior as in Y-Pr 1:2:3.

In brief, we could not observe any change in Raman and XPS of Y-Zn 1:2:3 samples. As Zn replaces Cu in the plane, it is possible that the B_{1g} mode ($\sim$340 cm^{-1}) and A_{1g} mode ($\sim$430 cm^{-1}) of plane oxygens show changes in their Raman frequencies. However, these two modes are quite broad so that we were unable to resolve any change in the frequency. For the Er-Pr 1:2:3 system on the other hand, we observed increases in the Raman frequency of the apical oxygen (O_z) stretching mode. The XPS spectra of the Er-Pr 1:2:3 system show that the binding energies of Ba 3*d* and 4*d* lines of the 1:2:3 phase increase as the Pr concentration increases. These observations for Er-Pr 1:2:3 are quite similar to those for Y-Pr 1:2:3 despite the differences in the relative strength of the magnetic moment of Y-site ions in the (1:2:3)-type superconductors. We conclude that the suppression mechanism in Er-Pr 1:2:3 is the same as in Y-Pr 1:2:3 and can be explained within the frame of the hole-localization scheme suggested for the Y-Pr 1:2:3 and Eu-Pr 1:2:3 systems.[13] Results of our experiments point out that the suppression mechanism in the Y-Zn 1:2:3 system may not be the same as that in Pr-substituted (1:2:3)-type superconductors.

II. EXPERIMENT

The $YBa_2Cu_{3-x}Zn_xO_7$ (x =0.0, 0.025, 0.06, 0.09) and $Er_{1-y}Pr_yBa_2Cu_3O_7$ (y =0.0, 0.1, 0.2, 0.3, 0.4) samples in our studies were prepared by the solid-state reaction method. Stoichiometric amounts of high-purity oxide powders were well mixed, pressed into pellets, and heated at 930 °C for 40 h in air, followed by annealing at 750 °C and 550 °C in flowing oxygen each for 12 h. The samples were then cooled slowly in the furnace to room temperature. The resultant pellets were reground thoroughly and the forementioned procedure was repeated two times. The x-ray-powder-diffraction patterns showed that all samples were of orthorhombic structure with little impurity. The measured lattice parameters are tabulated in Table I for both sample systems. The values for oxygen contents of $YBa_2Cu_{3-x}Zn_xO_7$ compounds were measured, after x-ray-powder-diffraction measurements, by the iodometric titration method and found to be 6.90±0.03 for all samples. This indicates that substitution of Zn by Cu does not affect oxygen content significantly. We have not included an analysis of the oxygen content of Er-Pr 1:2:3 compounds. It has been reported by several groups that the Pr content does not affect the oxygen content essentially in rare-earth 1:2:3.[14] The transition temperature T_c was determined from resistivity measurements by the standard four-probe technique using a high-precision *LCR* meter at a frequency of 23 Hz. Values of T_c determined by the midpoints of the resistivity data and the 10–90 % resistivity transition widths ΔT_c are also in Table I.

The microscopic Raman measurements were performed at room temperature using a Jobin Yvon U1000 double monochromator in a back-scattering geometry. The spectra were excited with an argon-ion laser operating at 514.5 nm and 488.0 nm wavelengths. The laser beam was focused onto a selected single crystal embedded in a freshly fractured surface of the ceramic samples. The incident laser beam was linearly polarized, and the intensity of the Raman-scattered light was analyzed in the same polarization of the incident beam. The spectrometer slit widths were 500 μm, which corresponds to a resolution of 2 cm^{-1} over the spectral range of interest. The Raman measurements were repeated several times at different crystallites of the sample to assure the reliability of our results. The spectra were taken over the range 100–700 cm^{-1}, scanning at 1.0 cm^{-1} step size with a time constant of 1 s. Care was taken not to heat the crystallites with the excessive power of the laser beam. The beam power of less than 1 mW was focused onto an area of 0.3×10^{-10} m^2.

The XPS measurements were done with the ESCA system manufactured by VSW Scientific Instruments in England, which is composed of three sectors of introduction, preparation, and main-analysis chambers. It is equipped

TABLE I. The lattice parameters determined by x-ray-powder diffraction, and the superconducting transition temperatures (T_c) and the 10–90 % transition widths (ΔT_c) determined by electrical resistivity measurements for (a) $YBa_2Cu_{3-x}Zn_xO_7$ and (b) $Er_{1-y}Pr_yBa_2Cu_3O_7$ samples.

(a)

x	a (Å)	b (Å)	c (Å)	$T_c[\Delta T_c]$ (K)
0.0	3.8201±0.0003	3.8853±0.0004	11.6893±0.0013	90.0[2.0]
0.025	3.8240±0.0003	3.8902±0.0004	11.6940±0.0012	73.5[6.3]
0.06	3.8188±0.0003	3.8877±0.0005	11.6665±0.0018	65.0[6.4]
0.09	3.8210±0.0003	3.8857±0.0003	11.6897±0.0011	52.8[8.0]

(b)

y	a (Å)	b (Å)	c (Å)	$T_c[\Delta T_c]$ (K)
0.0	3.8321±0.0016	3.9118±0.0041	11.7370±0.0032	90.8[0.7]
0.1	3.8345±0.0008	3.9167±0.0054	11.7581±0.0008	83.5[1.8]
0.2	3.8369±0.0017	3.9174±0.0045	11.7499±0.0036	70.5[2.1]
0.3	3.8432±0.0020	3.9172±0.0053	11.7406±0.0041	55.0[4.3]
0.4	3.8448±0.0014	3.9190±0.0039	11.7528±0.0030	41.2[5.6]

with a concentric hemispherical analyzer and a multichannel detector. We used monochromated Al $\kappa\alpha$ line ($h\nu = 1486.6$ eV) for the Y-Zn 1:2:3 system and unmonochromated Al $\kappa\alpha$ line for the Er-Pr 1:2:3 system as the x-ray source, and the pressure in the analysis chamber was maintained below 7.0×10^{-10} Torr during the XPS experiments. The analyzer was operated in the fixed-analyzer-transmission mode with a pass energy of 22 eV, which gave the overall instrumental resolution of 0.6 eV [full width at half maximum (FWHM)] for the Y-Zn 1:2:3 system and 1.0 eV for the Er-Pr 1:2:3 system including analyzer and source broadening. It should be noted here that the instrumental resolution is the capability of resolving two closely spaced peaks, not the limit by which we can determine the binding energies of the measured system. The method by which we determined the binding energies of Ba core levels is discussed in the result section. The absolute binding energy of the system was calibrated by measuring Cu $2p_{3/2}$ and Au $4f_{7/2}$ core levels of pure Cu and Au metals at the same time as our XPS experiments, whose binding energies are fixed at 932.7 and 84.0 eV, respectively.[15] In order to get the fresh surfaces of the samples, we scraped them *in vacuo* and measured all the major core levels immediately after the scraping.

III. RESULT

Figures 1 and 2 show representative Raman spectra of the Y-Zn 1:2:3 and Er-Pr 1:2:3 sample systems in $x(zz)\bar{x}$ polarization. Four Raman lines, A_{1g} in tetragonal notation, appear in all the Raman spectra. These modes have been assigned to the Ba and Cu stretching vibrations ($\sim$115 cm^{-1} and $\sim$150 cm^{-1}, respectively), the in-phase bond-bending vibration of the plane oxygens ($\sim$440 cm^{-1}), and the stretching vibration of the apical oxygens along the c axis ($\sim$500 cm^{-1}, hereafter O_z mode). The out-of-phase bond-bending vibration of the plane oxygens near 340 cm^{-1} is not allowed in this polarization. Impurity phases would show extra modes[16] at $\sim$640 cm^{-1} and $\sim$585 cm^{-1} for $BaCuO_2$ and $\sim$600 cm^{-1} and $\sim$390 cm^{-1} for Y_2BaCuO_5. As seen in Figs. 1 and 2, the spectra of our samples are relatively clean with no obvious impurity phase.

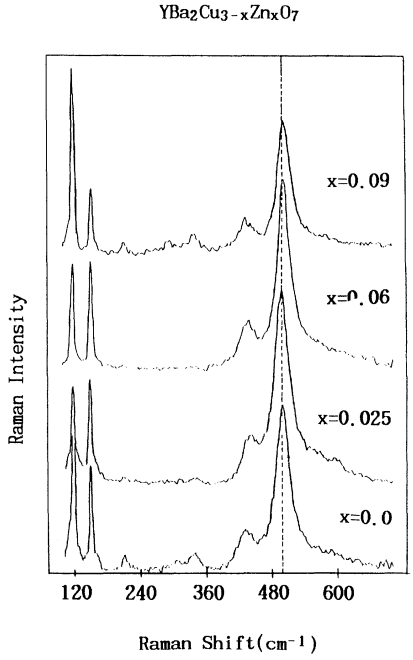

FIG. 1. Raman spectra of $YBa_2Cu_{3-x}Zn_xO_7$ samples in $x(zz)\bar{x}$ polarization. The dashed line, near the O_z mode, is a guide for the eye.

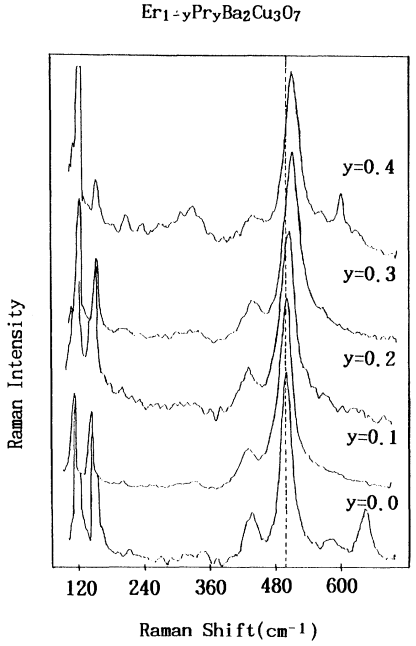

FIG. 2. Raman spectra of $Er_{1-y}Pr_yBa_2Cu_3O_7$ samples in $x(zz)\bar{x}$ polarization. The dashed line, near the O_z mode, is a guide for the eye.

The Raman frequencies of the O_z mode of Y-Zn 1:2:3 samples do not show any change with increasing Zn concentration. On the contrary, however, the Raman frequencies of the O_z mode of Er-Pr 1:2:3 increase by $\sim$8 cm^{-1} with increasing Pr concentration. All the other modes of both sample systems do not show any change within experimental resolution. In addition to the Raman lines, a sharp argon-plasma-discharge line appears in the spectra at 117 cm^{-1} when the 514.5 nm wavelength is used. To avoid such a plasma line near Ba-mode frequency, a 488.0 nm wavelength was used in determining the Ba mode. The Ba-mode peaks, not shown, taken using the 488.0 nm excitation line are rather broad and weak compared to another plasma line at 103 cm^{-1}, yet show such an increasing trend in frequency for the Er-Pr 1:2:3 system. The increase is about 2 cm^{-1} for $Er_{0.6}Pr_{0.4}Ba_2Cu_3O_7$, which is within the instrumental resolution.

The XPS spectra of all the samples were not significantly different from each other. The Ba $3d_{5/2}$ spectra of Y-Zn 1:2:3 are shown in Fig. 3. We have fitted

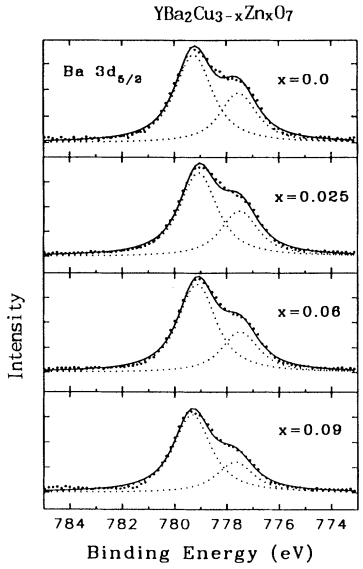

FIG. 3. XPS spectra of the Ba $3d_{5/2}$ for $YBa_2Cu_{3-x}Zn_xO_7$ ($x=0.0$, 0.025, 0.06, 0.09). Thick dots represent the raw data after subtraction of the inelastic background and the solid and dotted lines show the fitted results.

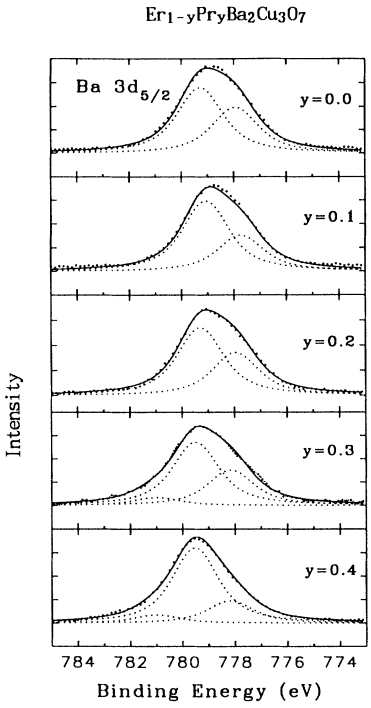

FIG. 4. XPS spectra of the Ba $3d_{5/2}$ for $Er_{1-y}Pr_yBa_2Cu_3O_7$ ($y=0.0$, 0.1, 0.2, 0.3, 0.4). Thick dots represent the raw data after subtraction of the inelastic background and the solid and dotted lines show the fitted results.

the Ba $3d_{5/2}$ spectra for each composition as shown in the figure. The FWHM of the Gaussian function due to the instrumental resolution was determined by fitting standard core-level peaks such as Ag $4f$, Ag $3d$, and Cu $2p$ of pure metals, whose intrinsic lifetime widths and singularity parameters are well known.[17] The higher binding energy peak of the Ba $3d_{5/2}$ shown in Fig. 3 originated from the nonsuperconducting phases such as $BaCO_3$, BaO, etc., which mainly reside on the surface of intrinsic superconducting granules. Its absolute binding energy is 779.5 eV, which is nearly the same as those of many literatures.[18,19] The other component at the lower binding-energy side is due to the intrinsic superconducting phase which includes the intrinsic surface component contributed from Ba atoms on the outermost layer, and the intrinsic bulk component from Ba atoms in the inner layers.[13,19] In the least-square fit, we fixed the line shapes of the extrinsic and intrinsic peaks, and changed the binding energies and the intensities of the two peaks. We have listed the binding energies of Ba $3d_{5/2}$ for the intrinsic component of Y-Zn 1:2:3 in Table II. The error in the absolute values of them is estimated to be within ± 0.1 eV. We can see that there are hardly any changes in these spectra independent of the composition.

The spectra of Ba $3d_{5/2}$ of Er-Pr 1:2:3 are shown in Fig. 4. In contrast to the case of Y-Zn 1:2:3 discussed above, we see a trend where core level of the intrinsic phase moves to a higher binding-energy side as y increases. To see this trend quantitatively, we have fitted the Ba $3d_{5/2}$ spectra as before. We then determined the binding energies of the intrinsic component of the Ba $3d_{5/2}$ for each composition of the Er-Pr 1:2:3 system, whose values are listed in Table III for comparison with those in Table II. A weak third component had to be introduced in the fit for the $y=0.3$ and 0.4 samples in order to keep consistency with the fitting of Ba $4d$ spectra (not shown). The component was negligible in the fit for other samples. This component seems to be from a minor amount of the $Ba(OH)_2$ impurity phase.[20] However, introduction of the third component should not affect the above results.

IV. DISCUSSION

We could not observe any change in Raman spectra and XPS of Y-Zn 1:2:3 samples. As Zn replaces Cu in the CuO_2 plane, it is possible that the B_{1g} mode (~ 340 cm^{-1}) and A_{1g} mode (~ 430 cm^{-1}) of plane oxygens

TABLE II. Binding energies of the intrinsic Ba $3d_{5/2}$ peaks for $YBa_2Cu_{3-x}Zn_xO_7$ ($x=0.0$ 0.025, 0.06, 0.09). The error in their values is within ± 0.1 eV.

x	0.0	0.025	0.06	0.09
Ba $3d_{5/2}$	777.5	777.5	777.5	777.7

TABLE III. Binding energies of the intrinsic Ba $3d_{5/2}$ peaks for $Er_{1-y}Pr_yBa_2Cu_3O_7$ ($y=0.0$, 0.1, 0.2, 0.3, 0.4). The error in their values is within ± 0.1 eV.

y	0.0	0.1	0.2	0.3	0.4
Ba $3d_{5/2}$	777.9	777.7	778.0	778.2	778.2

show changes in Raman frequencies. However, these two modes are quite broad that we were unable to resolve any change in the Raman frequency. Especially the Cu mode near 150 cm^{-1} was examined carefully and did not show any change. It could be argued that the maximum concentration of Zn tried in this work, 3 mole % of Cu, is simply too small to affect Raman spectra. Although this is quite plausible because of chemical and physical similarly between Cu and Zn ions, 3 mole % of Zn substitution for Cu is significant and comparable to 30 mole % of Pr substitution for Er in 1:2:3 superconductors as far as the suppression of the superconducting transition temperature is concerned (Table I). And we were rather interested in the effects of Zn substitution on Ba and O_z Raman modes in Y-Zn 1:2:3 superconductors.

On the other hand, Raman results of the Er-Pr 1:2:3 show an increase in frequency of the O_z mode with increasing Pr concentration. Similar behavior of the O_z mode was observed in the Y-Pr 1:2:3 system, where the Cu(1)-O_z bond length gets longer as the Pr concentration increases.[12] XPS results of the Er-Pr 1:2:3 show an increasing trend in binding energy of the Ba 3*d* core level with increasing Pr concentration. Both observations in Er-Pr 1:2:3 are similar to those for the Y-Pr 1:2:3 and Eu-Pr 1:2:3 systems.[12,13] Suppression of superconductivity occurs regardless of the relative magnitude of the magnetic moment of the Y-site ions replaced by Pr, indicating that the suppression may not be of magnetic origin as suggested by others.[21]

Superconductivity disappears at a larger concentration of Pr in the Y-Pr 1:2:3 than in Eu-Pr 1:2:3,[7,13] in which Eu-ion size is larger than Y-ion size. That is, the size of the cage consisting of the two nearest CuO_2 planes is larger for Eu 1:2:3 than for Y 1:2:3. Yet the effect of Pr substitution in suppression of superconductivity is stronger in Eu 1:2:3 than in Y 1:2:3. From these facts, suppression of superconductivity does not seem to correlate with mixing of the Pr 4*f* level with the CuO_2 plane.[22] Our argument contradicts that of Xu and Guan.[7]

However, the shifts of the Ba core levels and the frequency increases of the O_z and Ba Raman mode do correlate with suppression of superconductivity in the Pr-doped 1:2:3 systems. Thus, we believe that these shifts reflect changes in Ba-O overlap in the initial state. The shifts of the Ba core levels are considered to be due to an increase of localized holes with Ba 5*d* character as the Pr doping increases in Er-Pr 1:2:3 systems.[11,13] The frequency increases of the O_z and Ba Raman modes of the Er-Pr 1:2:3 system imply that the Ba-O bond gets hardened as the Pr concentration increases.[12,13] We conjecture that, as Pr concentration increases in the Er-Pr 1:2:3 system, charges are transferred from a Ba-O molecular band of strong Ba 5*d* character to a Ba-O bonding band such as Ba $6s-O\ 2p$.[13] This could result in effective hole localization at Ba sites in the Pr-doped 1:2:3 superconductors.

In summary, we have measured Raman spectra and XPS of $YBa_2Cu_{3-x}Zn_xO_7$ ($x=0.0$, 0.025, 0.06, 0.09) and $Er_{1-y}Pr_yBa_2Cu_3O_7$ ($y=0.0$, 0.1, 0.2, 0.3, 0.4) systems. For $YBa_2Cu_{3-x}Zn_xO_7$, no appreciable changes were observed. On the other hand, Ba and O_z Raman frequencies increase and the binding energies of Ba core levels shift to higher values as y increases in $Er_{1-y}Pr_yBa_2Cu_3O_7$. Results of our experiments point out that the suppression mechanism in the Y-Zn 1:2:3 system may not be the same as that in Pr-doped 1:2:3 systems. We conclude that the suppression mechanism in Er-Pr 1:2:3 is the same as that in Y-Pr 1:2:3 and can be explained within the frame of the hole-localization scheme suggested for the Y-Pr 1:2:3 and Eu-Pr 1:2:3 systems.[13] The Ba-O plane may play an important role in determining superconductivity via charge transfer between the CuO_2 plane and the Cu-O chain. It has been suggested that the Ba-O planes may play a role as charge reservoirs, which control the charge states of the CuO_2 planes.[23,24]

Recently, we noticed that Cohen *et al.*[25] reported no change in binding energies of Ba core levels in their XPS measurements on Y-Pr 1:2:3 samples annealed in oxygen *in situ*. However, it is known that annealing at high temperatures segregates surface components that are different from the bulk phase,[26] even though it cleans out an impurity phase such as $BaCO_3$. In the case of annealing in oxygen, an oxygen-rich surface phase might occur due to a surface barrier for oxygen indiffusion. Their value of binding energy of Ba $3d_{5/2}$ (779.2 eV), which is higher than ours ($\sim$777.7 eV), seems to support our point of view.

ACKNOWLEDGMENTS

I.-S.Y. appreciates the financial support (Grant Nos. 911-0206-010-2 and 92-25-00-02) of the Korea Science and Engineering Foundation, K.N. and C.K.K. acknowledge the financial support of the Ministry of the Science and Technology, Korea, S.-J.O. was supported in part by the Ministry of Science and Technology, Korea through the High-T_c Research Fund.

[1]G. Bednorz and K. A. Müller, Z. Phys. B **64**, 189 (1986).

[2]For example, R. Feile, Physica C **159**, 1 (1989).

[3]For example, G. Wendin, J. Phys. (Paris) Colloq. **48**, C9-483 (1987).

[4]J. D. Jorgensen, B. W. Veal, A. P. Paulikas, L. J. Nowicki, G. W. Crabtree, H. Claus, and W. K. Kwok, Phys. Rev. B **41**, 1863 (1990).

[5]W. E. Pickett, Rev. Mod. Phys. **61**, 433 (1989).

[6]There are many works regarding the Y-Zn 1:2:3 systems; we give only an example; M. W. Shafer, T. Penney, B. L. Olson, R. L. Greene, and R. H. Koch, Phys. Rev. B **39**, 2914 (1989).

[7]For example, Y. Xu and W. Guan, Phys. Rev. B **45**, 3176 (1992).

[8]B. Roughani, L. C. Sengupta, and W. C. H. Joiner, Physica C **171**, 77 (1990); Y. Xu, R. L. Sabatini, and K. W. Dennis, *ibid.* **169**, 205 (1990).

[9]The site that Zn ions go to remains to be resolved. However, the Cu(2) site is relatively well accepted. As an example, see

G. Roth, P. Adelmann, R. Ahrens, and B. Blank, Physica C **162-164**, 518 (1989).
[10]H. Zhenhui, Z. Han, S. Shifang, C. Zuyao, Z. Qirui, and X. Jiansheng, Solid State Commun. **66**, 1215 (1988); B. Jayaram *et al.* Phys. Rev. B **38**, 2903 (1988).
[11]In-Sang Yang, A. G. Schrott, and C. C. Tsuei, Phys. Rev. B **41**, 8921 (1990).
[12]In-Sang Yang, G. Burns, F. H. Dacol, and C. C. Tsuei, Phys. Rev. B **42**, 4240 (1990); In-Sang Yang, G. Burns, F. H. Dacol, J. F. Bringley, and S. S. Trail, Physica C **171**, 31 (1990).
[13]In-Sang Yang, A. G. Schrott, C. C. Tsuei, G. Burns, and F. H. Dacol, Phys. Rev. B **43**, 10 544 (1991).
[14]S. Martinez, A. Zwick, M. A. Renucci, R. Enjalbert, and P. Millet, Solid State Commun. **82**, 619 (1992).
[15]M. P. Seah, Surf. Interface Anal. **14**, 488 (1989).
[16]H. Rosen, E. M. Engler, T. C. Strand, V. Y. Lee, and D. Bethune, Phys. Rev. B **36**, 726 (1987); H. J. Rosen, R. M. Macfarlane, E. M. Engler, V. Y. Lee, and R. D. Jacowitz, *ibid.* **38**, 2460 (1988).
[17]P. H. Citrin, G. K. Wertheim, and Y. Bear, Phys. Rev. B **27**, 3160 (1983).
[18]X. D. Wu, A. Inam, M. S. Hegde, T. Venkatesan, C. C. Chang, E. W. Chase, B. Wilkens, and J. M. Tarascon, Phys. Rev. B **38**, 9307 (1988); J. Halbritter, P. Walk, H.-J. Mathes, B. Haeuser, and H. Rogalla, Z. Phys. B **73**, 277 (1988); H. Fjellvåg, P. Karen, A. Kjekshus, and J. K. Grepstad, Solid State Commun. **64**, 917 (1987).
[19]Moonsup Han, Se-Jung Oh, S. H. Moon, and Z-G. Khim (unpublished).
[20]J. Halbritter, P. Walk, H. -J. Mathes, B. Haeuser, and H. Rogalla, Z. Phys. B **73**, 277 (1988).
[21]C. S. Jee, A. Kebede, D. Nichols, J. E. Crow, T. Mihalisin, G. H. Myer, I. Perez, R. E. Salomon, and P. Schlottmann, Solid State Commun. **69**, 379 (1989).
[22]M. B. Maple, J. M. Ferreira, R. R. Hake, B. W. Lee, J. J. Neumeier, C. L. Seaman, K. N. Yang, and H. Zhou, J. Less-Common Met. **149**, 405 (1989).
[23]K. A. Müller, Z. Phys. B **80**, 193 (1990).
[24]R. J. Cava, Science **247**, 656 (1990).
[25]O. Cohen, F. H. Potter, C. S. Rastomjee, and R. G. Egdell, Physica C **201**, 58 (1992).
[26]A. G. Schrott, G. Singco, and K. N. Tu, Appl. Phys. Lett. **55**, 2126 (1989).